Monthly Notices
of the
ROYAL ASTRONOMICAL SOCIETY
MNRAS **445,** 3839–3847 (2014) doi:10.1093/mnras/stu1974

Red giant branch bump star counts in data and stellar models

David M. Nataf★
Research School of Astronomy and Astrophysics, The Australian National University, Canberra, ACT 2611, Australia

Accepted 2014 September 19. Received 2014 August 23; in original form 2014 July 16

ABSTRACT

We compare model predictions to observations of star counts in the red giant branch bump (RGBB) relative to the number density of first-ascent red giant branch at the magnitude of the RGBB, EW_{RGBB}. The predictions are shown to exceed the data by (5.2 ± 4.3) per cent for the BaSTI models and by (17.1 ± 4.3) per cent for the Dartmouth models, where the listed errors are purely statistical. These two offsets are brought to zero if the Galactic globular cluster metallicity scale is assumed to be overestimated by a linear shift of ∼0.11 and ∼0.36 dex, respectively. This inference based on RGBB star counts goes in the opposite direction to the increase in metallicities of Δ[M/H] ≈ 0.20 dex that would be required to fix the offset between predicted and observed RGBB luminosities. This comparison is a constraint on 'deep-mixing' models of stellar interiors, which predict decreased RGBB star counts. We tabulate the predictions for RGBB star counts as a function of [Fe/H], [α/Fe], CNONa, initial helium abundance, and age. Though our study suggests a small zero-point calibration issue, RGBB star counts should nonetheless be an actionable parameter with which to constrain stellar populations in the differential sense. The most significant outliers are towards the clusters NGC 5024 (M53), NGC 6723, and NGC 7089 (M2), each of which shows a ∼2σ deficit in their RGBB star counts.

Key words: stars: evolution – Hertzsprung–Russell and colour–magnitude diagrams – stars: luminosity function, mass function.

1 INTRODUCTION

The red giant branch bump (RGBB) is a feature of colour–magnitude diagrams (CMDs) of old ($t \gtrsim 1$ Gyr), well-populated stellar populations. As a star first ascends the red giant branch (RGB), the location of hydrogen burning in the star, a shell of mass (0.001–0.0001) $M_{\odot}$, moves outward with time as the star expands and grows more luminous. When the hydrogen-burning shell approaches the discontinuity in the hydrogen abundance near the maximum depth reached by the convective envelope, the luminosity of the star temporarily drops before increasing again, leading to an excess in the luminosity function (LF) over an underlying exponential distribution in magnitudes. This excess is referred to as the RGBB (Sweigart, Greggio & Renzini 1990; Cassisi & Salaris 1997; Bjork & Chaboyer 2006). The RGBB was first theoretically described by Thomas (1967) and Iben (1968). It was first empirically confirmed nearly two decades later, by King, Da Costa & Demarque (1985), in their observations of the globular cluster (GC) 47 Tuc. It has since been well documented that the characteristic luminosity (Fusi Pecci et al. 1990; Cassisi & Salaris 1997; Riello et al. 2003; Bjork & Chaboyer 2006; Di Cecco et al. 2010; Cassisi et al. 2011; Troisi et al. 2011), normalization (Bono et al. 2001; Riello et al. 2003; Bjork & Chaboyer 2006; Nataf et al. 2011a), and shape (Cassisi, Salaris & Bono 2002) of this excess are a steeply sensitive function of stellar models as well as assumed population parameters such as metallicity, age, and helium abundance.

There has been significant progress within the literature in tracking how the luminosity of the RGBB depends on metallicity, and by now a clear picture has emerged. When the RGBB is investigated in the Galactic GC population, the luminosity is found to steeply decline with metallicity (Piotto et al. 2002; Di Cecco et al. 2010; Cassisi et al. 2011; Troisi et al. 2011), at a rate of $dM_{V,\,RGBB}/d[M/H] = (0.737 \pm 0.024)$ mag dex^{-1} (Nataf et al. 2013) for a sample of Galactic GCs observed with the Wide Field and Planetary Camera 2 (WFPC2; Piotto et al. 2002) and Advanced Camera for Surveys (ACS; Sarajedini et al. 2007; Dotter, Sarajedini & Anderson 2011) Galactic GC treasury programs. A similar trend is also observed for nearby dwarf galaxies (Monelli et al. 2010).

However, though the existence of the RGBB and its approximate trend of luminosity with metallicity is a spectacular confirmation of stellar theory, there is one caveat: stellar models seemingly overpredict the luminosity of the RGBB in both Galactic GCs and dwarf spheroidal galaxies. The typical discrepancy measured is ∼0.20 mag, increasing to ∼0.40 mag for metallicities [M/H] = −2.00 and below. This has been confirmed whether one compares the brightness of the RGBB to that of the zero-age horizontal branch (ZAHB; Di Cecco et al. 2010), the main-sequence

★ E-mail: david.nataf@anu.edu.au

turn-off (Cassisi et al. 2011), or the brightness of the point on the main sequence at the same colour as the RGBB (Troisi et al. 2011). The combination of these three tests with their distinct systematics demonstrates that the discrepancy is not due to factors such as mass loss on the RGBB, incorrectly assumed ages, initial helium abundances, distances, or reddening estimates. Other possibilities, such as a large calibration error in the Galactic GC metallicity scale, or non-local overshoot at the base of the outer convective envelope (Alongi et al. 1991; Kamath, Karakas & Wood 2012) remain as plausible solutions, though the problem is not conclusively solved at this time.

This overprediction of the luminosity of the RGBB is thus a symptom of currently unspecified problems in either stellar models or how we interpret them (e.g. the assumed metallicity scale), and additional tests would thus be beneficial. An alternative to comparing luminosity measurements and predictions is to do the same for the normalization of the RGBB, i.e. the star counts, this would probe related physics but in principle have different sensitivities. Whereas the luminosity of the RGBB accounts for the *location* of the abundance discontinuity within the star, the normalization of the RGBB will be proportional to the *amplitude* of that discontinuity (Bono et al. 2001; Bjork & Chaboyer 2006), as the decreased molecular weight will slow down the efficiency of nuclear burning.

The comparison between RGBB star counts in models and data has previously been looked at (Bono et al. 2001; Piotto et al. 2002; Bjork & Chaboyer 2006), where agreement between theory and observation was found. However, there has since been an evolution in the Galactic GC metallicity scale (Carretta et al. 2009b). Further, there has been a vast improvement in both the quality and the quantity of the available photometric data (Sarajedini et al. 2007; Dotter et al. 2010) as well as in the methodology employed to measure the RGBB (Nataf et al. 2013). The combination of these two factors should lead to a $\sim$300 per cent increase in total effective precision. There is thus sufficient incentive to revisit the issue.

In addition to these factors, the Galactic GC system from which the bulk of the data for RGBB studies derive has been shown in the past decade to be more complex than previously believed. Many – perhaps all – GCs have a diverse star formation history, with some GCs showing spectacular variations in CNO and initial helium abundances, such as ω Centauri (Norris 2004) and NGC 2808 (Piotto et al. 2007). This may allow further testing of RGBB physics as continuously improving CMDs of these GCs better separate the distinct RGBs, and thus allow measurements of two (or more) distinct RGBBs. Indeed, Nataf et al. (2011b) reported a gradient in $\mathrm{EW}_{\mathrm{RGBB}}$ and I_{RGBB} towards 47 Tuc consistent with a helium-enhanced second generation being more centrally concentrated, i.e. the RGBB towards the inner part of 47 Tuc appeared slightly brighter and less well populated. Though the difference in helium between the first and second generation of 47 Tuc is not large ($\Delta Y \sim 0.02$; see Milone et al. 2012), the cluster is well populated and has very low differential reddening, allowing precise measurements of relatively small changes.

In this investigation we tabulate predicted values of RGBB star counts by means of its equivalent width on the red giant (RG) LF, $\mathrm{EW}_{\mathrm{RGBB}}$, from the BaSTI isochrones (Pietrinferni et al. 2004). We compare these to the values in a sample of 44 Galactic GCs where the RGBB's properties were measured by Nataf et al. (2013).

2 DATA

The data used by this investigation are that of 44 'gold-sample' measurements of $\mathrm{EW}_{\mathrm{RGBB}}$ with 1σ errors from Nataf et al. (2013), where the methodology is to be found in section 3 of that investigation. Following that paper, RGBB parameters from the GCs NGC 2808, 5286, 6388, and 6441 are excluded from the analysis due to the confounding issue of potentially very distinct multiple stellar populations within each of those clusters. These measurements were made on data from the *Hubble Space Telescope* (*HST*) treasury programs of Piotto et al. (2002), Sarajedini et al. (2007), and Dotter et al. (2011). We list the data in Table 1 and we plot its scatter in Fig. 1.

3 MODELS

We primarily use isochrones downloaded from the BaSTI stellar data base[1] (Pietrinferni et al. 2004; Cordier et al. 2007). Our tests span a broad range of input physics, including those that are α-enhanced (Cassisi et al. 2004; Pietrinferni et al. 2006), modified helium abundances, modified ages, and that have modified CNONa mixtures (Pietrinferni et al. 2009) as per recent observations of Galactic GCs. The CNONa-enhanced mixture changing the effective mass ratios of C:N:O:Na:Fe from 0.11:0.035:1:0.0013:0.032 to 0.18:14:1:0.052:0.30, in other words, significant increases in carbon, nitrogen, and sodium relative to oxygen, with the fraction of the total mass of metals locked up in the elements CNONa rising from 88 to 93 per cent. We also look at some extreme metallicities for the sake of completeness (Pietrinferni et al. 2013).

Models from the Dartmouth stellar data base (Dotter et al. 2008) are also used as a theoretical comparison over the full metallicity space of the Galactic GC system and for standard ages and chemical mixtures. Those predictions are listed in Table 3.

For each isochrone, we sample the LF in the magnitude range $I_{\mathrm{RGBB}} - 1.50 \leq I \leq I_{\mathrm{RGBB}} + 1.0$. We assume a Salpeter initial mass function (Salpeter 1955) such that $N(m) \propto m^{-2.35}$ when constructing the LF. An exponential is fit to the LF outside the RGBB, we then subtract this fit from the RGBB, measure the excess, and divide this excess by the best-fitting number density of underlying RG stars at the luminosity of the RGBB. This yields a predicted value of $\mathrm{EW}_{\mathrm{RGBB}}$ in a manner analogous to how astronomers routinely measure equivalent widths in stellar spectra. This process is further explained in Fig. 2. Some related LF parameters for some of these isochrones were calculated and summarized by Nataf, Cassisi & Athanassoula (2014).

3.1 The effect of varying the total metallicity [M/H]

What we have found is that the total metallicity [M/H] and the initial helium abundance Y have a substantial effect on the predicted value of $\mathrm{EW}_{\mathrm{RGBB}}$, whereas the age t/Gyr and the details of the metallicity mixture ([α/Fe] and CNONa variations at fixed total [M/H]) have minor effects. In Table 2, we summarize the predicted values of $\mathrm{EW}_{\mathrm{RGBB}}$ over a broad range of metallicities ($-2.27 \leq$ [M/H] $\leq +0.40$) for standard α-element, helium, and CNONa abundances, and an age t = 12 Gyr thought to be typical of Galactic GCs (Marín-Franch et al. 2009; Dotter et al. 2010), we also plot the predicted LFs in Fig. 3. The expectation is from an increase of $\mathrm{EW}_{\mathrm{RGBB}} = 0.146$ mag at [M/H] $= -2.27$ to $\mathrm{EW}_{\mathrm{RGBB}} = 0.429$ mag at [M/H] $= +0.06$, with $\mathrm{EW}_{\mathrm{RGBB}}$ then reaching a plateau maintained up to the highest metallicity probed [M/H] $= +0.40$. No simple predicted relationship can be written down for the dependence of $\mathrm{EW}_{\mathrm{RGBB}}$ as it is clearly curvilinear,

[1] http://basti.oa-teramo.inaf.it

Table 1. Summary of empirical values used in this work. Maximum likelihood values of the equivalent width of the RGBB, EW_{RGBB}, along with 1σ upper and lower bounds are taken from the investigation of Nataf et al. (2013), which is based on *HST* photometry from Piotto et al. (2002), Sarajedini et al. (2007), and Dotter et al. (2011). GC metallicities are taken from Carretta et al. (2009b), except for that of Lynga 07 which is taken from Bonatto & Bica (2008).

Cluster name	[M/H]	$\sigma_{[M/H]}$	EW_{RGBB}	EW^{+}_{RGBB}	EW^{-}_{RGBB}
LYNGA 07	−0.38	0.11	0.412	0.522	0.313
NGC 104 (47 Tuc)	−0.45	0.05	0.322	0.364	0.282
NGC 362	−1.09	0.07	0.306	0.379	0.249
NGC 1261	−1.02	0.10	0.213	0.273	0.146
NGC 1851	−0.90	0.10	0.294	0.363	0.236
NGC 3201	−1.27	0.05	0.477	0.666	0.300
NGC 5024 (M53)	−1.79	0.11	0.089	0.133	0.053
NGC 5272 (M3)	−1.26	0.07	0.249	0.324	0.196
NGC 5634	−1.66	0.11	0.272	0.421	0.146
NGC 5824	−1.67	0.15	0.212	0.284	0.153
NGC 5904 (M5)	−1.05	0.05	0.290	0.357	0.224
NGC 5927	−0.06	0.09	0.433	0.541	0.340
NGC 5986	−1.37	0.10	0.235	0.353	0.179
NGC 6093 (M80)	−1.58	0.10	0.152	0.211	0.109
NGC 6139	−1.44	0.11	0.273	0.362	0.204
NGC 6171 (M107)	−0.66	0.07	0.599	0.883	0.387
NGC 6205 (M13)	−1.36	0.07	0.218	0.283	0.165
NGC 6218 (M12)	−1.03	0.06	0.312	0.425	0.208
NGC 6229	−1.17	0.11	0.273	0.398	0.197
NGC 6254 (M10)	−1.30	0.05	0.316	0.425	0.219
NGC 6284	−1.06	0.10	0.305	0.437	0.192
NGC 6304	−0.14	0.09	0.320	0.418	0.249
NGC 6341 (M92)	−2.01	0.07	0.157	0.228	0.105
NGC 6352	−0.48	0.07	0.403	0.593	0.248
NGC 6356	−0.12	0.15	0.327	0.394	0.268
NGC 6362	−0.82	0.07	0.426	0.600	0.297
NGC 6402 (M14)	−1.13	0.11	0.272	0.357	0.195
NGC 6541	−1.50	0.10	0.237	0.316	0.148
NGC 6569	−0.48	0.15	0.429	0.544	0.326
NGC 6584	−1.24	0.11	0.214	0.301	0.132
NGC 6624	−0.19	0.09	0.433	0.531	0.350
NGC 6637 (M69)	−0.37	0.09	0.303	0.383	0.223
NGC 6638	−0.74	0.09	0.307	0.419	0.216
NGC 6652	−0.52	0.15	0.416	0.598	0.229
NGC 6681 (M70)	−1.36	0.10	0.290	0.393	0.187
NGC 6723	−0.72	0.09	0.188	0.256	0.137
NGC 6752	−1.23	0.05	0.430	0.571	0.286
NGC 6760	−0.17	0.15	0.470	0.586	0.368
NGC 6864 (M75)	−1.04	0.15	0.387	0.473	0.323
NGC 6934	−1.30	0.11	0.211	0.311	0.139
NGC 6981	−1.22	0.09	0.415	0.566	0.293
NGC 7006	−1.20	0.08	0.318	0.387	0.245
NGC 7078 (M15)	−2.04	0.08	0.173	0.233	0.120
NGC 7089 (M2)	−1.36	0.09	0.129	0.163	0.097

however, over the range $-1.79 \leq [\mathrm{M/H}] \leq -0.25$, it can be approximated by

$$\mathrm{EW}_{\mathrm{RGBB}} \approx 0.185 + 0.0732([\mathrm{M/H}] + 1.79) + 0.0411([\mathrm{M/H}] + 1.79)^2. \quad (1)$$

For real observations the detectability of the RGBB is expected to increase with metallicity at a rate higher than the factor of 0.429/0.146–300 per cent one might naively infer from the numbers reported in the previous paragraph. In addition to this factor, the RGBB actually becomes fainter by ~2 mag and is thus shifted to a region of the RGB where stellar evolution is slower, and thus the underlying continuum against which we measure EW_{RGBB} is itself increasing. The actual increase in RGBB star counts between those two metallicities ([M/H] = −2.27, +0.06) should be of a factor of ~10.

We also looked at the model predictions from the Dartmouth stellar data base (Dotter et al. 2008), with the results listed in Table 3. A comparison of the two curves can be found in the top panel of Fig. 4. The predictions from the Dartmouth models are systematically higher than those from the BaSTI models by ~0.03 mag, with the offset being nearly consistent over the full range of metallicities. As BaSTI and Dartmouth assume similar values of the mixing length ($\alpha_{ML} = 1.91, 1.94$), the helium-enrichment ratio ($dY/dZ = 1.4, 1.5$), the primordial helium abundance ($Y_{BB} = 0.245, 0.245$), and the same opacities it is not clear why the predictions differ. Weiss et al.

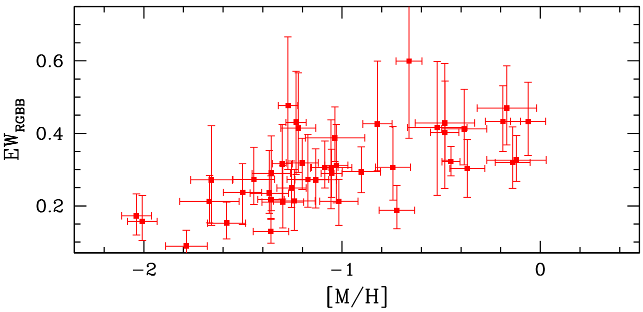

Figure 1. The trend of the equivalent width of the RGBB, EW_{RGBB}, versus metallicity. Empirical values (red squares) and corresponding error bars are from Nataf et al. (2013).

(2007) noted that numerical issues may play a role, with the Dartmouth models predicting an RGBB luminosity ∼0.10 mag brighter than the FRANEC models (basis for the BaSTI data base) even if all the parameters are fixed to be at the same value.

3.2 The effect of varying the initial helium abundance *Y*

The second most significant effect is that of variations in the initial helium abundance *Y*. In Table 4, we summarize the predicted effect on EW_{RGBB} of increasing *Y* for four different metallicities. Increasing *Y* is predicted to decrease the value of EW_{RGBB}. At [M/H] = −2.27, the expectation is from an decrease of $EW_{RGBB} = 0.146$ at $Y = 0.245$ to $EW_{RGBB} = 0.053$ at $Y = 0.400$. The fractional decrease remains high though is a little slower at [M/H] = +0.06, where the expectation is from an decrease of $EW_{RGBB} = 0.429$ at $Y = 0.273$ to $EW_{RGBB} = 0.220$ at $Y = 0.400$. The predicted relationship can be summarized as follows:

$$\frac{\mathrm{d}\,EW_{RGBB}}{\mathrm{d}Y} \approx -[0.85 + 0.49([M/H] + 1.79)]. \qquad (2)$$

It will be interesting to see if this prediction is verified in Galactic GCs as multicolour photometry continues to refine the splits in RGBs due to metallicity, CNONa abundances, helium, etc. This decrease in EW_{RGBB} with increasing *Y* is in addition to the fact that

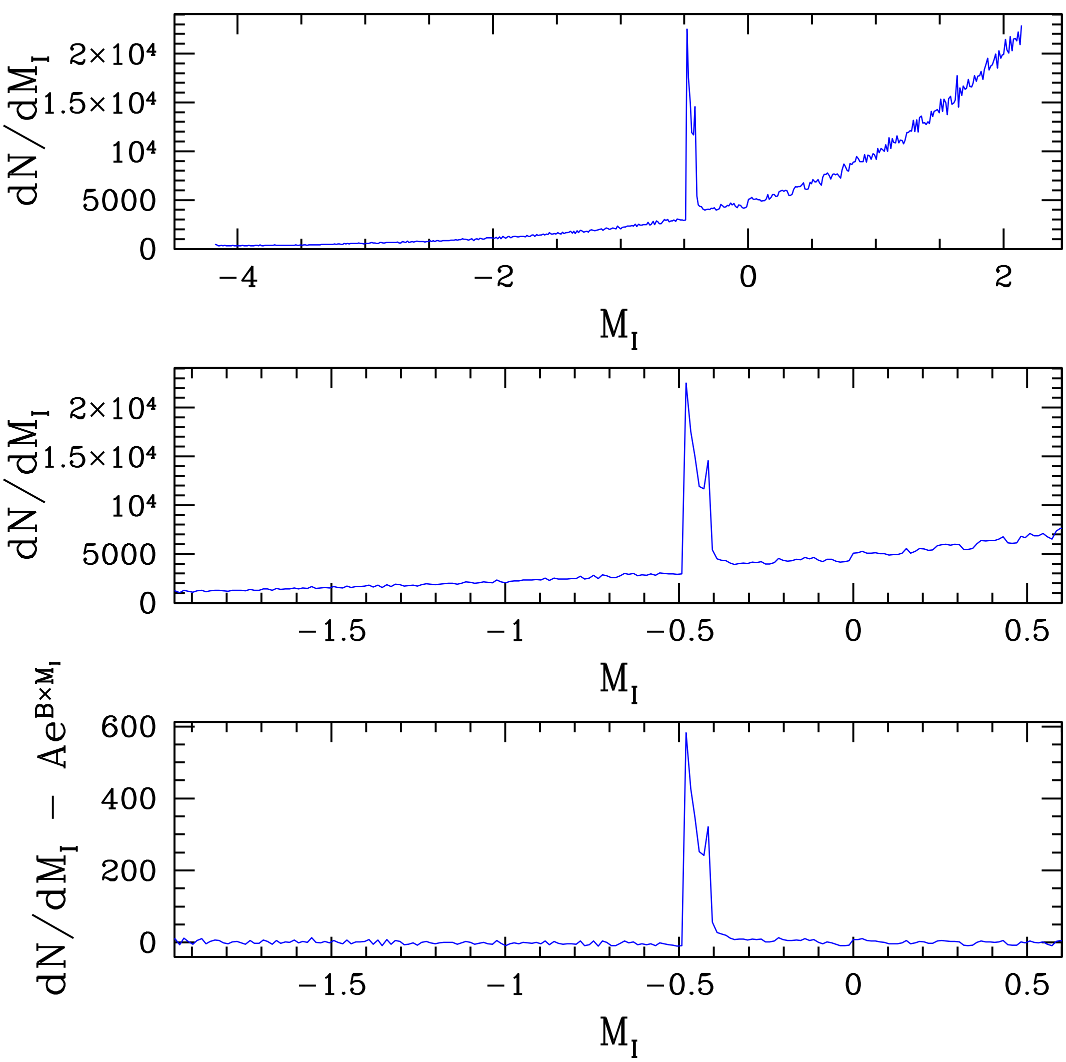

Figure 2. The BaSTI LF (Pietrinferni et al. 2004) for an [M/H] = −0.963, [α/Fe] = 0.00, $t = 12$ Gyr isochrone with standard helium and CNONa abundances. This isochrone has a predicted exponential slope of $B = 0.735$, $M_{I,\,RGBB} = -0.45$, and $EW_{RGBB} = 0.291$. Top: the LF in the range $-4.18 \le M_I \le 2.14$, over which the exponential form of the underlying red giant LF away from the RGBB is easily discernible. Middle: the LF over the range $I_{RGBB} - 1.50 \le I \le I_{RGBB} + 1.0$, which is where we compute our fits. Bottom: residuals to the LF with an exponential fit to the underlying RGB subtracted. The residuals are consistent with zero away from the RGBB. The two peaks in the LF correspond to the brightest and faintest parts of the RGBB, the reader may find a detailed discussion of the shape of the RGBB in Cassisi et al. (2002).

Table 2. Predicted RGBB equivalent width, EW_{RGBB} for standard Galactic GC ages and chemistries over a broad range of metallicities, calculated from BaSTI isochrones (Pietrinferni et al. 2004), as a function of the metallicity [M/H], [α/Fe] fixed to standard values, the age $t = 12$ Gyr, and the initial helium abundance Y fixed to scaled solar, integrated in the luminosity range $I_{RGBB} - 1.50 \le I \le I_{RGBB} + 1.0$.

[M/H]	[α/Fe]	Y	t (Gyr)	EW_{RGBB}
−2.27	+0.40	0.245	12	0.146
−1.79	+0.40	0.245	12	0.185
−1.49	+0.40	0.246	12	0.212
−1.27	+0.40	0.246	12	0.232
−0.96	+0.40	0.248	12	0.276
−0.66	+0.40	0.251	12	0.320
−0.35	+0.40	0.256	12	0.375
−0.25	+0.40	0.259	12	0.396
+0.06	0.00	0.273	12	0.429
+0.25	0.00	0.288	12	0.425
+0.40	0.00	0.303	12	0.417

increasing Y raises the luminosity of the RGBB ($dM_I/dY \sim -3.0$), shifting the RGBB to a region of slightly faster evolution, as well as the fact that the total normalization of the RGB lifetime decreases with increasing Y at a rate of $\Delta \log\, t_{RGB} \sim -0.84 \Delta Y$ (Renzini 1994). The combination of these two factors should decrease the RGBB star counts by ~35 per cent for a change of $\Delta Y = +0.10$, in addition to the effect of a decreased EW_{RGBB}.

3.3 The effect of varying the age at fixed metallicity

The models predict that age variations at the level observed in Galactic GCs should yield a minor impact on measurements of EW_{RGBB}. We show predicted EW_{RGBB} for four representative metallicities and ages $t = 4$, 7, 10, 12, and 14 Gyr in Table 5. Decreasing age is predicted to increase EW_{RGBB} at low metallicity. At [M/H] = −0.35, this trend begins to reverse, with EW_{RGBB} decreasing between $t = 7$ and 4 Gyr, and for [M/H] = +0.25 the peak in EW_{RGBB} is reached in the age range $10 < t/\mathrm{Gyr} < 14$.

For the age range $10 < t/\mathrm{Gyr} < 14$, which is the one relevant to Galactic GCs (Marín-Franch et al. 2009; Dotter et al. 2010), the predicted relationship can be summarized as follows:

$$\frac{d\,EW_{RGBB}}{dt} \approx -0.016 + 0.0065([\mathrm{M/H}] + 2.27). \quad (3)$$

3.4 The effect of varying the metals mixture at fixed total [M/H]

It is well-documented that Galactic GCs host stars of varying chemical mixtures, both in terms of α-elements (Carretta et al. 2009a) and CNONa mixtures (Ivans et al. 1999; Yong et al. 2009; Marino et al. 2011). Fixing the total value of [M/H] is to fix the number of metallic ions relative to hydrogen, it does not necessarily mean that stellar structure should stay the same in all cases (in fact it does not), as different metallic species can contribute differently to the opacity of star, as well as be thermonuclear catalysts. We thus investigate the effect of varying [α/Fe] at fixed [M/H], summarized in Table 6, and of varying CNONa at fixed [M/H], summarized in Table 7. We find that for both cases EW_{RGBB} is predicted to be nearly independent of the metals mixture.

A decrease in [α/Fe] of 0.40 dex, coupled to an increase in [Fe/H] of ~0.29 dex such that [M/H] is fixed, does increase EW_{RGBB}, but barely so. The predicted shift ΔEW_{RGBB} is never higher than ~0.015 mag, and typically ~0.005 mag. Similarly, increasing CNONa at fixed [M/H] such that [Fe/H] decreases by 0.27 dex does increase EW_{RGBB} is small, though larger than for shifts due to α-enhancement. The predicted shift is $\Delta EW_{RGBB} = +0.018$ mag at [M/H] = −1.79 and $\Delta EW_{RGBB} = -0.036$ mag at [M/H] = −0.35. For both cases, the predicted shift is vastly smaller than the median measurement error of ~0.08 mag reported by Nataf et al. (2013). The takeaway is that EW_{RGBB} will depend far more on the total metallicity than on the details of the metals mixture.

4 EW_{RGBB} IN DATA VERSUS MODELS

In Fig. 4 we plot the measured and predicted EW_{RGBB} in the top panel, with the residuals relative to the BaSTI models obtained when one subtracts the predicted from the measured values in the middle and bottom panels, all as a function of [M/H].

The weighted linear least-squares fit yields an offset relative to the BaSTI models of

$$EW_{RGBB,(data-predicted)} = (-0.014 \pm 0.011) + (0.002 \pm 0.021)([\mathrm{M/H}] + 1.0216)), \quad (4)$$

and relative to the Dartmouth models of

$$EW_{RGBB,(data-predicted)} = (-0.045 \pm 0.011) + (0.001 \pm 0.021)([\mathrm{M/H}] + 1.0216)), \quad (5)$$

in other words, the observed EW_{RGBB} are smaller than the predicted values, by a small (0.014 ± 0.011) mag in the BaSTI models and by (0.045 ± 0.011) in the Dartmouth models. The trend with metallicity is consistent with zero for both sets of models.

These results undermine the possibility that the offset between predicted and observed RGBB luminosities is due to a calibration error in the metallicity scale of Galactic GCs. That problem, viewed in isolation, could be resolved if the metallicity scale of Galactic GCs (Carretta et al. 2009b) *underestimated* metallicities. However, an analogously perfect match RGBB star count predictions and observations would require that the metallicity scale *overestimate* metallicities. The offsets relative to the BaSTI and Dartmouth predictions would, respectively, be brought to zero if the Galactic GC metallicity scale is assumed to be overestimated by a linear shift of ~0.11 and ~0.36 dex. A shift in the metallicity scale is thus not a viable proposition for the data and model offset in RGBB physics.

4.1 A note on comparing EW_{RGBB} in data and models in light of the error in predicted RGBB luminosities

The naive 'null hypothesis' one should first attempt is a straight-up comparison between the predicted and observed values of EW_{RGBB}, However, as noted in the Introduction, it is by now well-documented that theory overestimates the luminosity of the RGBB by a typical value of ~0.20 mag, reaching ~0.40 mag in the most metal-poor clusters (Di Cecco et al. 2010; Cassisi et al. 2011; Troisi et al. 2011). If one were to then assume that what theory should predict is the *integrated luminosity* of the RGBB, one might then shift the comparison point.

A coincidental cancellation ends up mitigating this concern. As the RGBB is observed to take place at a magnitude ~0.20 mag dimmer than predicted by models, the assumption of fixed integrated luminosity would yield a duration for this phase of stellar evolution

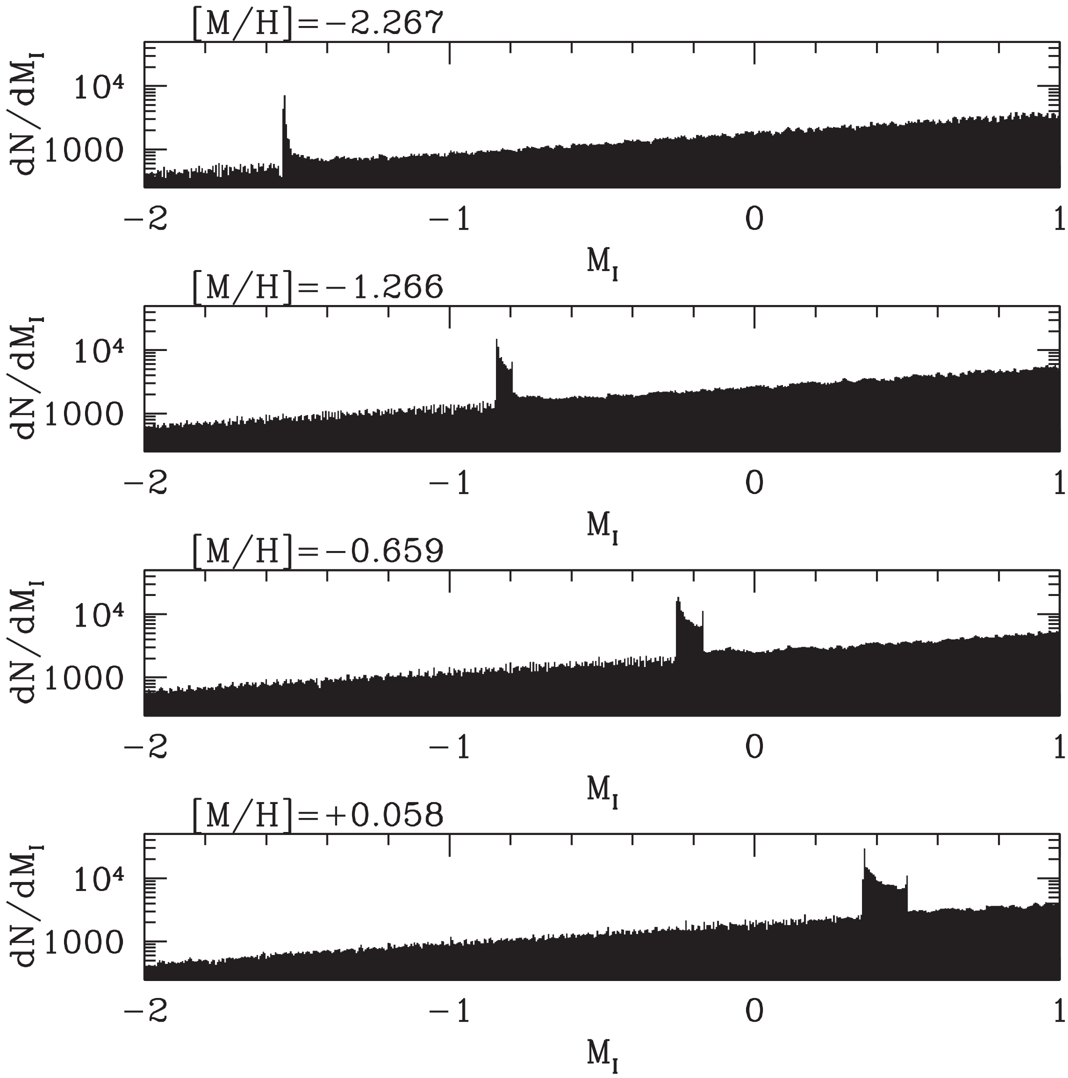

Figure 3. The BaSTI LF (Pietrinferni et al. 2004) for $t = 12$ Gyr, [α/Fe]=+0.40 for the RGB. As the metallicity varying from [M/H] = −2.267 in the top panel to [M/H] = +0.058 in the bottom panel, the normalization of the RGBB increases from $\mathrm{EW_{RGBB}} = 0.146$ to 0.424. This increased normalization is in addition to the underlying normalization of the RGB at the location of the bump itself increasing.

Table 3. Predicted RGBB equivalent width, $\mathrm{EW_{RGBB}}$ for standard Galactic GC ages and chemistries over a broad range of metallicities, calculated from Dartmouth isochrones (Dotter et al. 2008). Symbols and methodology as in Table 2.

[M/H]	[α/Fe]	Y	t (Gyr)	$\mathrm{EW_{RGBB}}$
−2.20	+0.40	0.245	12	0.168
−1.70	+0.40	0.246	12	0.228
−1.20	+0.40	0.247	12	0.269
−0.70	+0.40	0.251	12	0.344
−0.20	+0.40	0.262	12	0.438
+0.07	0.00	0.274	12	0.461
+0.21	0.00	0.286	12	0.462
+0.36	0.00	0.301	12	0.459
+0.56	0.00	0.329	12	0.429

extended by ∼17 per cent relative to model predictions. However, the RGB against which $\mathrm{EW_{RGBB}}$ is normalized is denser at these magnitudes, by an approximate factor exp(0.73 × 0.20) = 1.16, or 16 per cent, which nearly perfectly offsets the aforementioned 17 per cent. The respective numbers are 31 and 34 per cent if one assumes a 0.40 mag offset, once again similar.

This cancellation is due to the fact that the exponential component of the RG LF goes as $N(m) \propto \exp(0.73 M_{\mathrm{Bol}}) \approx 10^{(0.32\, M_{\mathrm{Bol}})}$ (Castellani, Chieffi & Norci 1989; Nataf et al. 2013), whereas luminosities go as $L \propto 10^{-0.40\, M_{\mathrm{Bol}}}$. These two effects combine for a distortion of $\sim 10^{0.08 \Delta M_{\mathrm{Bol}}}$, where ΔM_{Bol} is the offset between predicted and observed magnitudes, which is smaller than 10 per cent for offsets of $\Delta M \leq 0.50$ mag.

4.2 A note on comparing $\mathrm{EW_{RGBB}}$ in data and models in light of multiple stellar populations

The anonymous referee expressed concern about the possible role of multiple stellar populations in affecting the results and interpretations here. We have excluded four GCs from our analysis (NGC 2808, 5286, 6388, and 6441) but there is a possibility that other GCs might have just as much internal diversity.

We recognize this concern, and that it is possible that in the future there will be a need to revisit this analysis for these reasons.

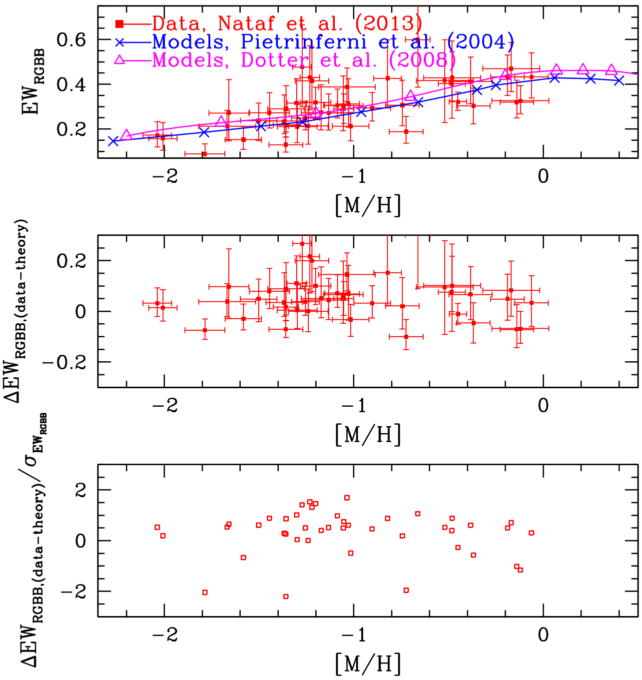

Figure 4. Top: the trend of the equivalent width of the RGBB, $\mathrm{EW_{RGBB}}$, versus metallicity. Empirical values (shaded red squares) are from Nataf et al. (2013), and the theoretical values under the assumption of $t = 12$ Gyr and a standard elemental mixture are taken from the BaSTI stellar data base (blue X's; Pietrinferni et al. 2004) and the Dartmouth stellar data base (unshaded magenta triangles; Dotter et al. 2008). Model predictions are interpolated by cubic spline. Middle: residuals when the predicted $\mathrm{EW_{RGBB}}$ are subtracted from the observed values. Bottom: residuals from the middle panel, with their values divided by the error taking the asymmetry of the error bars into account.

Table 4. Predicted RGBB equivalent width, $\mathrm{EW_{RGBB}}$, for four metallicities, standard ages, and metallicities, but over a range of initial helium abundances. Symbols and methodology as in Table 2.

[M/H]	[α/Fe]	Y	t (Gyr)	$\mathrm{EW_{RGBB}}$
−1.79	+0.40	0.245	12	0.185
−1.79	+0.40	0.300	12	0.094
−1.79	+0.40	0.350	12	0.080
−1.79	+0.40	0.400	12	0.053
−0.96	+0.40	0.248	12	0.276
−0.98	+0.40	0.300	12	0.201
−0.96	+0.40	0.350	12	0.147
−0.96	+0.40	0.400	12	0.100
−0.35	+0.40	0.256	12	0.375
−0.35	+0.40	0.300	12	0.296
−0.35	+0.40	0.350	12	0.237
−0.35	+0.40	0.350	12	0.159
+0.06	+0.40	0.273	12	0.424
+0.07	+0.40	0.350	12	0.289
+0.06	+0.40	0.400	12	0.220

As analytical methods improve, more GCs might turn out to be more challenging to interpret. Yong et al. (2013) recently measured an intrinsic spread of σ[Fe/H] ≈ 0.03 dex for NGC 6752. That is too small to affect interpretations of the RGBB, but in principle the same methodology could be applied to other clusters leading to larger measured spreads that would matter. Indeed, Yong et al. (2014) measured a much larger variation for NGC 7089 (M2). They found that four of 14 stars (29 per cent) from their biased sample had their metallicity enhanced from [Fe/H] ≈ −1.7 (the mode of the cluster metallicity distribution function) to [Fe/H] ≈ −1.0. This would in principle explain the underpopulated RGB bump of NGC 7089 as a number of the stars would be undergoing the RGBB phase at a different luminosity. However, Piotto et al. (2012) showed, using a photometric analysis of the subgiant branch, that only ∼5 per cent of the stars in that cluster belonged to the extreme population, which is too small to noticeably affect our results. Indeed, $\mathrm{EW_{RGBB,NGC\,7089}} = 0.129 \pm 0.033$, whereas the predicted value for [M/H] = −1.36 is $\mathrm{EW_{RGBB}} = 0.223$ for the BaSTI models and $\mathrm{EW_{RGBB}} = 0.254$ for the Dartmouth models. The offset is closer to 50 per cent than it is to 5 per cent, thus there may be another factor at play, or simply a statistical fluke. The GCs NGC 5024 (M53) and NGC 6723 show comparable deficiencies in their RGBB star counts to NGC 7089 (M2), and thus may warrant precision abundance investigations.

Table 5. Predicted RGBB equivalent width for four metallicities but over a range of ages. Symbols and methodology as in Table 2.

[M/H]	[α/Fe]	Y	t (Gyr)	$\mathrm{EW_{RGBB}}$
−1.79	+0.40	0.245	14	0.137
−1.79	+0.40	0.245	12	0.185
−1.79	+0.40	0.245	10	0.211
−1.79	+0.40	0.245	7	0.260
−1.79	+0.40	0.245	4	0.327
−0.96	+0.40	0.248	14	0.259
−0.96	+0.40	0.248	12	0.276
−0.96	+0.40	0.248	10	0.314
−0.96	+0.40	0.248	7	0.336
−0.96	+0.40	0.248	4	0.374
−0.35	+0.40	0.256	14	0.364
−0.35	+0.40	0.256	12	0.375
−0.35	+0.40	0.256	10	0.389
−0.35	+0.40	0.256	7	0.401
−0.35	+0.40	0.256	4	0.375
+0.25	0.00	0.288	14	0.423
+0.25	0.00	0.288	12	0.425
+0.25	0.00	0.288	10	0.421
+0.25	0.00	0.288	7	0.398
+0.25	0.00	0.288	4	0.307

Table 6. Predicted RGBB equivalent width as α-abundances are decreased and Fe-abundances increased at fixed [M/H]. Symbols and methodology as in Table 2.

[M/H]	[α/Fe]	Y	t (Gyr)	$\mathrm{EW_{RGBB}}$
−1.79	+0.40	0.245	12	0.185
−1.79	0.00	0.245	12	0.188
−0.96	+0.40	0.248	12	0.276
−0.96	0.00	0.248	12	0.291
−0.35	+0.40	0.256	12	0.375
−0.35	0.00	0.256	12	0.382
+0.25	+0.40	0.288	12	0.424
+0.25	0.00	0.288	12	0.425

We showed in Section 3.4 that varying the metals mixture at fixed total metallicity has little impact on $\mathrm{EW_{RGBB}}$. With that said, one should maintain awareness of these variations when measuring RGBB parameters. First of all, CNONa does not vary at fixed [M/H],

Table 7. Predicted RGBB equivalent width for four different representative combinations of initial helium abundance and [M/H], but each with different combination having two different partitions between CNONa and Fe with the total metallicity fixed. Symbols and methodology mostly as in Table 2, we also list [Fe/H] and CNONa status.

[M/H]	[Fe/H]	[α/Fe]	CNONa extreme	Y	t (Gyr)	EW_{RGBB}
−1.79	−2.14	+0.40	No	0.245	12	0.185
−1.79	−2.41	+0.40	Yes	0.245	12	0.180
−0.96	−1.31	+0.40	No	0.248	12	0.276
−0.96	−1.58	+0.40	Yes	0.248	12	0.257
−0.96	−1.31	+0.40	No	0.350	12	0.147
−0.96	−1.58	+0.40	Yes	0.350	12	0.139
−0.35	−0.70	+0.40	No	0.256	12	0.375
−0.35	−0.97	+0.40	Yes	0.256	12	0.321

but rather at fixed [Fe/H], as such the CNONa-enhanced population will be [M/H]-enhanced and will thus be expected to have more densely populated RGBBs. Further, though EW_{RGBB} is predicted to be largely insensitive to the details of the metals mixture, $M_{I,\,RGBB}$ is not. Decreasing [α/Fe] by 0.40 dex at fixed [M/H] dims the RGBB by a measurable $\Delta M_{I,\,RGBB} \sim 0.07$ mag, whereas increasing CNONa brightens the RGBB by ∼0.03 mag at [M/H] = −1.79, and by a much larger ∼0.17 mag at [M/H] = −0.35. These shifts are sufficiently large that they can either distort the shape of the RGBB or even split it into separate RGBBs localized at separate luminosities, necessitating care in analysis. Once again, as more data emerge on the multiple populations in Galactic GCs, there may be a need for a re-analysis of RGBB physics in data and models.

5 DISCUSSION AND CONCLUSION

We have compiled the best literature data available on EW_{RGBB} (Nataf et al. 2013), a parameter of star counts on the RGBB, and compared these to predictions from the BaSTI stellar data base (Pietrinferni et al. 2004). We have found that the offset between data and theory is small, $EW_{RGBB,\,(data\text{-}predicted)} = (0.014 \pm 0.011)$, consistent with zero for the BaSTI models, with the offset rising to $EW_{RGBB,\,(data\text{-}predicted)} = (0.045 \pm 0.011)$ for the Dartmouth models.

These results constrain suggested solutions to the issue of the offset between predicted and observed RGBB luminosities in Galactic GCs (Di Cecco et al. 2010; Cassisi et al. 2011; Troisi et al. 2011). That problem cannot be resolved by assuming an error in the adopted metallicity scale, as a systematic shift as small as 0.16 dex in [M/H] (not sufficient to resolve the luminosity discrepancy) would yield a $\geq 3\sigma$ offset between measured and predicted EW_{RGBB}. The issue is thus more likely to be one pertaining to the *physics* of stellar models, such as the treatment of convection, as suggested by Alongi et al. (1991) and Kamath et al. (2012).

Looking to the horizon, we see the prospects for improved data from Galactic GCs as marginal, as the existing surveys are already accomplished (Piotto et al. 2002; Sarajedini et al. 2007; Dotter et al. 2011). There may be opportunities for improved measurements of Galactic bulge GCs as multicolour photometry comes in allowing a treatment of the substantial differential reddening observed towards the inner Galaxy, thus constraining the behaviour of the RGBB at higher metallicities. We argue that this consistency increases confidence in RGBB star counts as an actionable parameter with which to constrain the nature of stellar populations, see also Nataf et al. (2011a,b). The theoretical predictions listed within this work extend beyond the age–helium–metallicity space spanned by the Galactic GC system, and thus can be of use to other kinds of observation, for example that of LFs investigated towards the *Kepler* field (Hekker et al. 2011).

ACKNOWLEDGEMENTS

I thank Martin Asplund, Santi Cassisi, and Aaron Dotter for helpful discussions. I also thank the anonymous referee for a helpful report. Author was supported by the Australian Research Council grant FL110100012. This work has made use of BaSTI web tools.

REFERENCES

Alongi M., Bertelli G., Bressan A., Chiosi C., 1991, A&A, 244, 95
Bjork S. R., Chaboyer B., 2006, ApJ, 641, 1102
Bonatto C., Bica E., 2008, A&A, 479, 741
Bono G., Cassisi S., Zoccali M., Piotto G., 2001, ApJ, 546, L109
Carretta E., Bragaglia A., Gratton R., Lucatello S., 2009a, A&A, 505, 139
Carretta E., Bragaglia A., Gratton R., D'Orazi V., Lucatello S., 2009b, A&A, 508, 695
Cassisi S., Salaris M., 1997, MNRAS, 285, 593
Cassisi S., Salaris M., Bono G., 2002, ApJ, 565, 1231
Cassisi S., Salaris M., Castelli F., Pietrinferni A., 2004, ApJ, 616, 498
Cassisi S., Marín-Franch A., Salaris M., Aparicio A., Monelli M., Pietrinferni A., 2011, A&A, 527, A59
Castellani V., Chieffi A., Norci L., 1989, A&A, 216, 62
Cordier D., Pietrinferni A., Cassisi S., Salaris M., 2007, AJ, 133, 468
Di Cecco A. et al., 2010, ApJ, 712, 527
Dotter A., Chaboyer B., Jevremović D., Kostov V., Baron E., Ferguson J. W., 2008, ApJS, 178, 89
Dotter A. et al., 2010, ApJ, 708, 698
Dotter A., Sarajedini A., Anderson J., 2011, ApJ, 738, 74
Fusi Pecci F., Ferraro F. R., Crocker D. A., Rood R. T., Buonanno R., 1990, A&A, 238, 95
Hekker S. et al., 2011, A&A, 530, A100
Iben I., 1968, Nature, 220, 143
Ivans I. I., Sneden C., Kraft R. P., Suntzeff N. B., Smith V. V., Langer G. E., Fulbright J. P., 1999, AJ, 118, 1273
Kamath D., Karakas A. I., Wood P. R., 2012, ApJ, 746, 20
King C. R., Da Costa G. S., Demarque P., 1985, ApJ, 299, 674
Marín-Franch A. et al., 2009, ApJ, 694, 1498
Marino A. F., Villanova S., Milone A. P., Piotto G., Lind K., Geisler D., Stetson P. B., 2011, ApJ, 730, L16
Milone A. P. et al., 2012, ApJ, 744, 58
Monelli M., Cassisi S., Bernard E. J., Hidalgo S. L., Aparicio A., Gallart C., Skillman E. D., 2010, ApJ, 718, 707
Nataf D. M., Udalski A., Gould A., Pinsonneault M. H., 2011a, ApJ, 730, 118
Nataf D. M., Gould A., Pinsonneault M. H., Stetson P. B., 2011b, ApJ, 736, 94

Nataf D. M., Gould A. P., Pinsonneault M. H., Udalski A., 2013, ApJ, 766, 77
Nataf D. M., Cassisi S., Athanassoula E., 2014, MNRAS, 442, 2075
Norris J. E., 2004, ApJ, 612, L25
Pietrinferni A., Cassisi S., Salaris M., Castelli F., 2004, ApJ, 612, 168
Pietrinferni A., Cassisi S., Salaris M., Castelli F., 2006, ApJ, 642, 797
Pietrinferni A., Cassisi S., Salaris M., Percival S., Ferguson J. W., 2009, ApJ, 697, 275
Pietrinferni A., Cassisi S., Salaris M., Hidalgo S., 2013, A&A, 558, A46
Piotto G. et al., 2002, A&A, 391, 945
Piotto G. et al., 2007, ApJ, 661, L53
Piotto G. et al., 2012, ApJ, 760, 39
Renzini A., 1994, A&A, 285, L5
Riello M. et al., 2003, A&A, 410, 553
Salpeter E. E., 1955, ApJ, 121, 161
Sarajedini A. et al., 2007, AJ, 133, 1658
Sweigart A. V., Greggio L., Renzini A., 1990, ApJ, 364, 527
Thomas H. C., 1967, Z. Astrophys., 67, 420
Troisi F. et al., 2011, PASP, 123, 879
Weiss A., Cassisi S., Dotter A., Han Z., Lebreton Y., 2007, in Vazdekis A., Peletier R. F., eds, Proc. IAU Symp. 241, Stellar Populations as Building Blocks of Galaxies. Cambridge Univ. Press, Cambridge, p. 28
Yong D., Grundahl F., D'Antona F., Karakas A. I., Lattanzio J. C., Norris J. E., 2009, ApJ, 695, L62
Yong D. et al., 2013, MNRAS, 434, 3542
Yong D. et al., 2014, MNRAS, 441, 3396

This paper has been typeset from a TEX/LATEX file prepared by the author.